

Fundamental and practical aspects of reactive N_2^+ -ion sputtering in Auger in-depth analysis

T. Kawabata and F. Okuyama^{a)}

Applied Physics Laboratory, Department of Systems Engineering, Nagoya Institute of Technology, Gokiso-cho, Showa-ku, Nagoya 466, Japan

M. Tanemura

Toyota Central Research and Development Laboratories, Inc., 41-1, Aza Yokomichi, Oaza Nagakute, Nagakute-cho, Aichi-gun, Aichi-ken 480-11, Japan

(Received 22 October 1990; accepted for publication 18 December 1990)

Polycrystalline Al, Mo, Ti, and Ta films deposited on Si wafers were systematically depth profiled by Auger electron spectroscopy using Ar^+ and N_2^+ ions as projectile. In agreement with the traditional concept of reactive sputtering, N_2^+ sputtering of Al and Mo films textured the surface less, thereby improving depth resolution significantly.

N_2^+ -sputtered Ti and Ta films, on the other hand, were characterized by microprojections thickly covering the bombarded area, forming a striking contrast to Ar^+ -sputtered Ti and Ta displaying less-enhanced surface texturing. As revealed by electron spectroscopy for chemical analysis, the N_2^+ -bombarded surface was nitrified for every material, and the nitride zone was confined to the surface or near-surface for Al and Mo and extended far below the surface for Ti and Ta. It is thus considered that three-dimensional nitridation lay under the enhanced surface texturing observed for N_2^+ -sputtered Ti and Ta.

I. INTRODUCTION

Auger electron spectroscopy (AES) combined with inert-gas ion sputtering is the most popular existing technique for compositional analysis of solid surfaces and solid-solid interfaces. In so-called Auger depth profiling, the degree of conformity between the true and measured profiles is described in terms of Auger depth resolution. Unfortunately, bombarding inert-gas ions texture the surface, thereby causing a serious deterioration in depth resolution, especially for polycrystalline metal targets.¹⁻⁷ Thus, a way to minimize the ion-induced surface texturing has long been a problem in surface science and thin-film technology.

One means to approach the above goal is to use chemically active ions, typically N_2^+ ions, as projectiles: sputtering with N_2^+ ions, for example, has been supposed to reduce surface texturing, and hence improve depth resolution, for most metallic materials.⁷⁻¹¹ A widely accepted view is that the reduction in surface texturing associated with N_2^+ sputtering is due to the chemical bond formation between target and implanted nitrogen atoms, but very little evidence⁷ has been presented so far in support of this theory.

In general, Auger depth resolution is increased by lowering sputtering energy. According to the "shrapnel" model proposed by Zalm and Beckers,¹² the main effect of using molecular-ion projectiles is to lower the sputtering energy through the disruption of impacting ions. In this model, the prime cause of the resolution improvement attainable with N_2^+ should be the reduction in effective sputtering energy, not the chemical bond formation. Currently, there is no consensus as to whether N_2^+ ions improve the depth resolution chemically or physically. What is also

unknown is whether or not N_2^+ sputtering invariably reduces the surface texturing. To provide satisfactory answers to these questions, the morphological, structural, and chemical features of N_2^+ -sputtered surfaces must be studied systematically, as a function of target material.

II. EXPERIMENT

A. AES, SEM, and ESCA

The samples subjected to surface characterization are listed in Table I, together with their dimensional details. Also presented in the table are the nitrides of the respective sample materials and their heat of formation.¹³ The samples were polycrystalline films of Al, Mo, Ti, and Ta deposited on mirror-polished (100) Si wafers using a dc sputtering technique. (The polycrystallinity of the films was confirmed by x-ray diffraction.) As seen from the table, the nitrides of these metals possess negative heats of formation: the metals should react with atomic nitrogen without an external heat supply. Typical as-prepared samples observed by scanning electron microscopy (SEM) are shown in Fig. 1. The Al surface was far from smooth, consisting of well-developed crystallites, whereas the Ti and Ta surfaces were ideally smooth. The Mo surface possessed an intermediate roughness. The film-substrate interface was thought to be as flat as the substrate surface. By AES, the samples were determined to be virtually impurity free.

Every sample was bombarded with Ar^+ and N_2^+ ions in a JAMP-10S scanning Auger microprobe equipped with a microbeam ion gun. The incident angle of the ion beam was 60° with respect to the surface normal. The ion current density and the ion energy were usually regulated to ~ 100

^{a)}To whom correspondence should be addressed.

TABLE I. Samples used in this study and the heat of formation of their nitrides (H_f) at 25 °C.¹³

| Material | Thickness (nm) | Nitride | H_f (kcal g ⁻¹ mol ⁻¹) |
|----------|----------------|-------------------|---|
| Al | 300 | AlN | - 57.7 |
| Mo | 300 | Mo ₂ N | - 8.3 |
| Ti | 100 | TiN | - 73.0 |
| Ta | 300 | TaN | - 58.2 |

Film substrate, mirror-polished (100) Si wafer.

$\mu\text{A}/\text{cm}^2$ and 3 keV, respectively, but in some cases Ar^+ ions were accelerated to 1.5 keV, in order to confirm the physical effect of N_2^+ sputtering. The ion beam was focused into a microbeam $\sim 150 \mu\text{m}$ across, which allowed us to produce two craters or more on the same target (Fig. 2). No mass separation was done in N_2^+ sputtering, but the nitrogen ions impinging on the sample should mostly have been N_2^+ , because of the well-known cracking pattern of molecular nitrogen (N_2^+ -to- N^+ ratio, about 10). The energy, absorbed current, and electron-beam diameter in Auger analysis were 10 keV, 100 nA, and 400 nm, respectively. On depth profiling, the normally incident electron beam was carefully adjusted to the center of the ion-impacted area. The background pressure in the analyzing chamber was lower than 1×10^{-7} Pa, and the chamber stayed in the 10^{-6} Pa region even during sputtering, owing to differential pumping of the ion gun. The purities of Ar and N_2 gases were higher than 99.999%.

To determine the topographical change due to ion sputtering, the depth-profiled samples were observed by high-resolution SEM, using an ISI-DS130 electron microscope. The chemical state of sputtered surfaces was also examined *in situ*, by means of electron spectroscopy for chemical analysis (ESCA) (ESCA LAB MARK-II system). The x-ray excitation was done with the $\text{MgK}\alpha$ line, and the measurements were carried out in the constant analyzer mode, with the pass energy adjusted to 20 eV. The operating pressure of the analyzer was in the 10^{-8} Pa region, which was low enough to avoid the impurity adsorption on the measured surface.

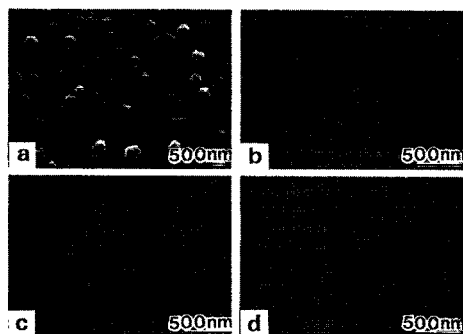


FIG. 1. Typical as-deposited surfaces of (a) Al, (b) Mo, (c) Ti, and (d) Ta films, observed by high-resolution SEM. The viewing direction was 40° with respect to surface normal.

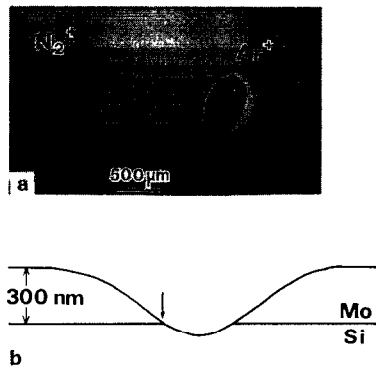


FIG. 2. (a) Low-magnification SEM image of craters produced on an Mo film by 3-keV Ar^+ and N_2^+ ions. (b) Schematic representation of the crater cross section. The arrow in (b) indicates the area examined by high-resolution SEM.

B. TEM

The sample materials employed are so reactive with nitrogen that their interaction with energetic nitrogen ions should lead to the nitridation of the area exposed to the ion flux. If so, a question arises: how deep is the nitrided zone? Since answering this is very informative for discussing the fundamental aspects of reactive N_2^+ sputtering, the bulk structural change caused by N_2^+ -ion impact was checked by transmission electron microscopy (TEM), for the respective sample materials. (ESCA is not available for this purpose, because of its information depth as shallow as $\sim 1.5 \text{ nm}^{14}$). To do so, rectangular platelets were cut out from Marz-grade polycrystalline sheets 0.05 mm thick, and then polished chemically at one edge, attaining razorlike configurations [Fig. 3(a)]. A platelet thus prepared was uprighted in the Auger microprobe, and its sharpened edge was bombarded with vertically incident N_2^+ ions under the sputtering conditions described earlier [Fig. 3(b)]. (Prior to ion bombardment, every sample was washed carefully in an ultrasonic cleaner.) After sputtering, the sample was transferred to a JEM-2000FX electron microscope, for determining the crystalline state of the bombarded area. Since the platelets were previously cut so as to be directly

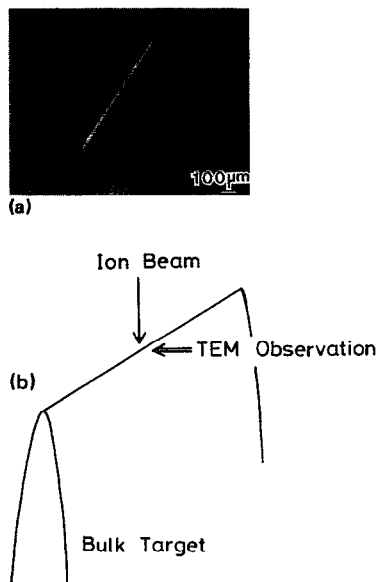


FIG. 3. (a) Low-magnification SEM image of a bulk sheet target. (b) Directions of ion-incidence and TEM observation for the target (schematic).

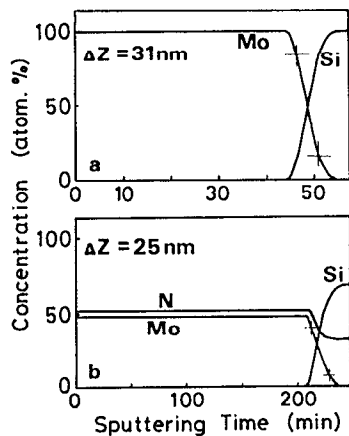


FIG. 4. Auger depth profiles for Mo (186 eV) corresponding to the craters in Fig. 2(a). (a) 3-keV Ar^+ sputtering, and (b) 3-keV N_2^+ sputtering. The crosses indicate the 84 and 16% levels of Mo intensity.

mountable on the sample stage of the electron microscope, sample-holding meshes were unnecessary for their observation.

III. RESULTS

Figure 4 shows Auger depth profiles for an Mo film bombarded with 3-keV Ar^+ and N_2^+ ions, indicating the variation of element concentration with sputtering time. (The element concentration was calculated using the relative element sensitivity factors tabulated in Ref. 15.) Note that the nitrogen signal was detected during the sputter removal of the Mo layer. This suggests the chemical bond formation between molybdenum and implanted nitrogen atoms.⁷ The depth profiles for the other materials attained by N_2^+ sputtering also comprised the nitrogen signal, so we may conclude that N_2^+ sputtering of the present materials entailed chemical processes more or less.

The depth resolution, Δz , for the profiles recorded was evaluated on the basis of the "two standard deviation." In this definition, the depth resolution is given by the difference of the depth coordinate between 84% and 16% (the crosses in Fig. 4) of the intensity change at the interface.¹⁶ The values of depth resolution thus evaluated for thin films sputtered with 3-keV Ar^+ and N_2^+ are listed in Table II, together with the sputtering time needed for the ion beam to reach the film-substrate interface. Table II shows that N_2^+ sputtering improved the resolution for Al and Mo, but led to less satisfactory resolutions for Ti and Ta. Thus, it

TABLE II. Auger depth resolutions Δz obtained with 3-keV Ar^+ and N_2^+ sputtering, and sputtering times t needed for the ion beam to reach the film-substrate interface. Auger depth profiles for KLL Al (1396 eV), MNN Mo (186 eV), LMM Ti (387 eV) and NNN Ta (179 eV) signals were used to evaluate the resolutions.

| Ion species | Δz (nm) | | t (min) | |
|-------------|-----------------|----------------|---------------|----------------|
| | Ar^+ | N_2^+ | Ar^+ | N_2^+ |
| Al | 107 | 46 | 64 | 346 |
| Mo | 31 | 25 | 48 | 224 |
| Ti | 17 | 25 | 21 | 80 |
| Ta | 8 | 13 | 73 | 267 |

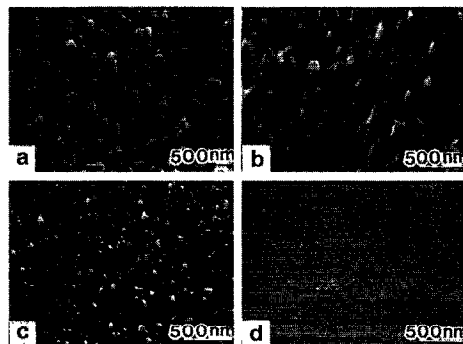


FIG. 5. Topographical structures of Ar^+ -sputtered (a) Al, (b) Mo, (c) Ti, and (d) Ta surfaces, in the proximity of film-substrate interface (high-resolution SEM images). Ion energy: 3 keV.

turned out that reactive N_2^+ sputtering is not always superior to Ar^+ sputtering in resolving depth profiles. In addition, N_2^+ sputtering needed a long time for one run: typically, the sputtering time to remove a 100 nm thickness of Ti was 80 min for 3-keV N_2^+ , which was about four times longer than that for 3-keV Ar^+ . Such a long analysis time prevents the practical application of N_2^+ sputtering to Auger in-depth analysis.

The prime factors to govern Auger depth resolution are (i) atomic mixing and (ii) radiation-induced surface texturing. For polycrystalline metal targets, the latter effect is far more dominant,¹⁻⁸ so that the resolutions listed in Table II should reflect the degree of roughness of sputtered surfaces. Figure 5 shows the SEM images of the walls of craters formed on Al, Mo, and Ti surfaces bombarded with 3-keV Ar^+ , and indicates the morphological structures in the proximity of the film-substrate interface [see Fig. 2(b)]. It is seen that the sample surfaces, except for Ta, were heavily textured, with conical protrusions grown thickly. The average cone dimension decreased in the order of Al, Mo, and Ti, agreeing very well with the resolution increase in the same order. The sputtered Ta surface exhibited no texturing detectable by SEM, and this nontextured surface was no doubt responsible for a high depth resolution (8 nm) attained for Ta. Shown in Fig. 6 are Al and Mo samples exposed to 1.5-keV Ar^+ ions. As determined by comparing these SEM images with Figs. 5(a) and 5(b), the average cone dimension was reduced very slightly by

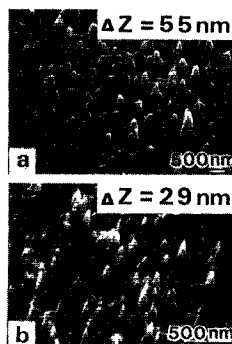


FIG. 6. Topographical structures of (a) Al and (b) Mo surfaces sputtered with 1.5-keV Ar^+ . Inset in the images are the corresponding depth resolutions.

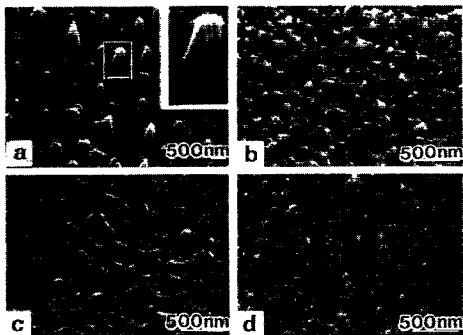


FIG. 7. Topographical structures of N_2^+ -sputtered (a) Al, (b) Mo, (c) Ti, and (d) Ta surfaces. Inset in (a) is an enlarged image of the area enclosed by the rectangle. Ion energy: 3 keV.

halving Ar^+ -ion energy. The corresponding depth resolutions, inset in the images, were better than the resolutions obtained with 3-keV Ar^+ , but they were definitely lower than those provided by 3-keV N_2^+ . Thus, the resolution improvement observed for N_2^+ -sputtered Al and Mo was not explicable in terms of the lowering of sputtering energy alone: chemical effects might have been involved in the N_2^+ sputtering processes of the metals.

Compared to Ar^+ sputtering, N_2^+ sputtering resulted in less-enhanced surface roughening for Al and Mo. As seen in Fig. 7(a), the Al surfaces sputtered with 3-keV N_2^+ were typically characterized by cone bunches (note area enclosed by rectangle), the numerical density of which was a little lower than that of the cones formed on Ar^+ -sputtered Al. The protrusions developed on N_2^+ -sputtered Mo were much smaller than those formed by Ar^+ , and in addition they exhibited no definite configuration [Fig. 7(b)]. Without doubt, these less-textured surfaces of N_2^+ -sputtered Al and Mo were directly related to the corresponding depth resolution improved markedly.

It was mentioned already that N_2^+ sputtering of Ti and Ta resulted in resolution loss. Shown in Fig. 7(c) is a Ti sample sputtered with N_2^+ , which reveals thickly grown protrusions of undefined configurations. In harmony with the deteriorated depth resolution, these surface protrusions were much more macroscopic than the conical protrusions on Ar^+ -sputtered Ti. Also, their undefined configurations are an indication that the texturing of the Ti surface involved a bulk chemical process. (For the surface texturing due solely to sputter removal of surface atoms, the resulting protrusions are shaped conically.) A more surprising fact is that N_2^+ ions roughened the originally smooth Ta surfaces. As shown in Fig. 7(d), the Ta surfaces sputtered with N_2^+ consisted of fine protrusions, forming a striking contrast to the Ar^+ -sputtered Ta surfaces which maintained the original smoothness. In general, surface grains function as the nucleation sites of surface protrusions.^{17,18} This implies that fine-grained samples are less susceptible to ion-induced surface texturing. The textured surfaces of N_2^+ -sputtered Ta would therefore suggest that impacting N_2^+ ions caused the original surface grains to grow, providing the ground for surface texturing.

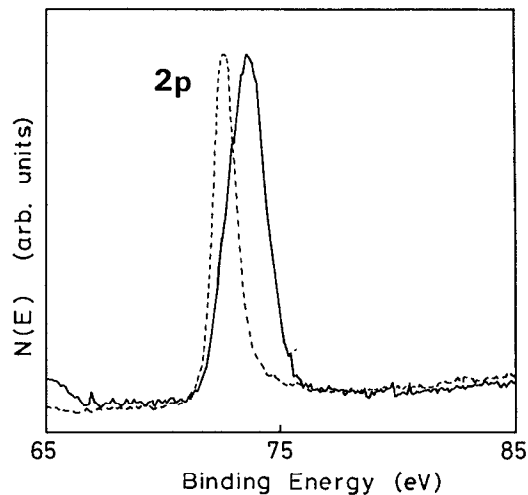


FIG. 8. ESCA spectra of Al films bombarded *in situ* with 40 keV Ar^+ (broken-line curve) and 4-keV N_2^+ (solid-line curve).

In the light of the Auger and SEM data cited above, N_2^+ sputtering of the present materials would presumably involve chemical processes. To ascertain this, thin film samples bombarded with 4-keV Ar^+ and N_2^+ ions were observed by ESCA. The result for Al is shown in Fig. 8, in which are depicted photoelectron peaks in the Al $2p$ region for N_2^+ -sputtered (full curve) and Ar^+ -sputtered (broken curve) films. The $2p$ signal from the Ar^+ -sputtered surface coincided with clean Al, thus displaying no chemical shift.¹⁹ The N_2^+ -sputtered surface, by contrast, gave rise to a $2p$ signal shifted to higher energy. The energy shift was estimated to be 1.25 eV, which means that the shifted peak was due to photoelectrons emitted from AlN.²⁰ The ESCA data for N_2^+ -sputtered Mo has been described elsewhere in detail.⁷ In brief, the chemical shift was too small to determine the chemical composition of nitride, perhaps indicating that the nitridation of the Mo surface was only partial.

The shift of ESCA signals was more distinct for Ti and Ta sputtered with N_2^+ . For Ti, the energy shift was 1.3 eV, which exactly corresponded to TiN (Fig. 9).¹⁹ Similarly, the Ta surface was entirely transformed into TaN by bombarding N_2^+ ions.

As already noted, accelerated N_2^+ ions were mostly dissociated into atomic nitrogen upon impact with the target,^{12,21} thereby implanting nitrogen atoms beneath the surface. Since the present metals are highly reactive with atomic nitrogen, these implanted nitrogen atoms readily reacted with neighboring metal atoms to form nitride in the near surface. In general, metal nitrides are stable chemically and possess very high melting points. The nitrides of Al, Mo, Ti, and Ta are no exception: they are all refractory materials and hence resistive to sputtering. The prolonged sputtering required for depth profiling with N_2^+ should be ascribable in part to the nonvolatility of the nitrides.

If the nitride formation associated with N_2^+ sputtering arises from the reaction between metal and implanted nitrogen atoms, the nitrided depth should be of the same

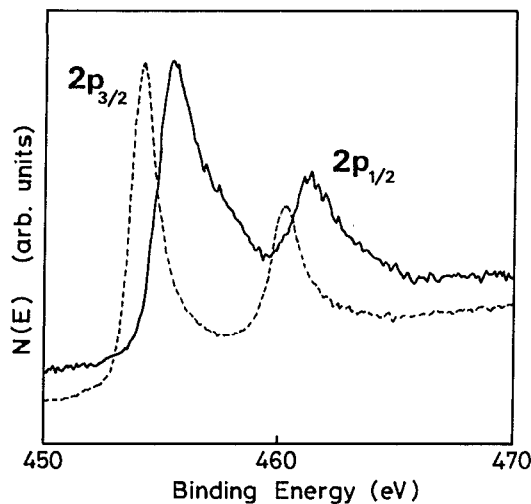


FIG. 9. ESCA spectra of Ti films bombarded *in situ* with 4-keV Ar^+ (broken-line curve) and 4-keV N_2^+ (solid-line curve).

order as the penetration depth of projectiles. The projected ranges of 3-keV N_2^+ , or 1.5 N^+ , hitting the present metals were calculated using the LSS theory,²² and the results are presented in Table III. These theoretical data suggest that the nitridation is confined to the near-surface region several nm thick. But this was not the case for Ti and Ta, as disclosed by TEM of N_2^+ -sputtered platelets. Figure 10 shows the TEM data of a Ti platelet exposed to N_2^+ ions for a prolonged period. The electron diffraction (ED) pattern of the edge area of the platelet consisted of regularly arranged spots [Fig. 10(b)], and the net formed by the spots was confirmed by careful analysis to match the (110) reciprocal lattice section of TiN. This assures that the sample edge was wholly nitrided into TiN. As clear in the dark-field image in Fig. 10(c), the components of the edge area were TiN crystallites with a preferred orientation: an oriented growth of TiN crystallites took place on the N_2^+ -sputtered area. Since the crystallite dimension amounted to 20 nm on the average, the nitrided zone extended far below the penetration depth of nitrogen atoms.

For Ta, too, evidence was obtained that the nitrided zone was thicker than the penetration depth of projectiles. However, ED patterns of N_2^+ -sputtered Al and Mo displayed no reflections from nitride (Fig. 11). For Al and Mo, the nitrided zone might have been too thin to diffract electrons.

TABLE III. Projected ranges R_p of normally incident 3-keV N_2^+ ions determined by LSS calculation.

| Target | R_p (nm) |
|--------|------------|
| Al | 4.5 |
| Mo | 2.3 |
| Ti | 4.4 |
| Ta | 1.3 |

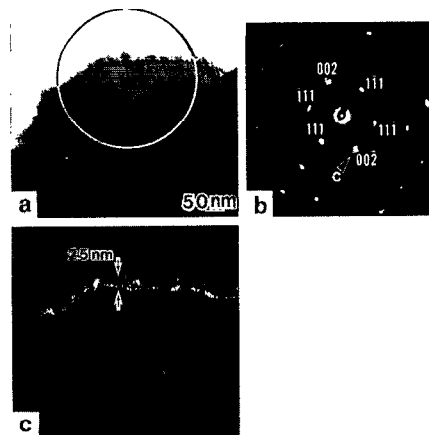


FIG. 10. TEM image of a Ti bulk target sputtered with 3-keV N_2^+ ions for 6 h. (a) Bright-field image, (b) ED pattern of the encircled area in (a), and (c) dark-field image produced by the spot C.

IV. DISCUSSION

The Auger, ESCA, and TEM observations described above may lead one to conclude that, as far as the present sample materials are concerned, N_2^+ sputtering involves the formation of metal-nitrogen bonds, in addition to the rupture of N—N bonds. The same conclusion has also been reached for Ag/Mo sandwiches bombarded with N_2^+ .⁷ Our new finding is that N_2^+ sputtering is inferior to Ar^+ sputtering, in relation to the resolution improvement for Ti and Ta. According to a current theory, the reactive sputtering generally reduces surface texturing,⁸⁻¹⁰ so N_2^+ sputtering of Ti and Ta should lead to a marked improvement in resolution. The present findings cast doubt on the validity of the theory.

Commonly, radiation-induced surface texturing is enhanced on polycrystalline targets, because crystallites on the virgin surface function as the nuclei of surface cones. Conversely speaking, surface texturing is less enhanced on targets with fine-grained structures. This common rule is clearly reflected in the less- and nontextured surfaces of the Ar^+ -bombarded Ti and Ta films [see Figs. 5(c) and 5(d)]. Disagreeing with the rule, however, the originally smooth Ti and Ta surfaces were heavily textured by N_2^+ ions. To reasonably interpret this finding, it must be hypothesized that impacting N_2^+ ions grew crystallites on Ti and Ta,



FIG. 11. TEM image of a Mo bulk target bombarded with 3-keV N_2^+ ions for 6 h. (a) Bright-field image and (b) corresponding ED pattern, showing the (100) reflection from the Mo lattice.

and eroded the surface as well. To view the TEM data in Fig. 10, the crystallites would belong to nitrides. In other words, the growth of nitride particles was behind the texturing of N_2^+ -sputtered Ti and Ta.

The most common primary ion species in secondary ion mass spectrometry (SIMS) is O_2^+ . Like N_2^+ , O_2^+ is said to be reactive and to produce smooth surfaces. According to a recent SIMS study by Moens *et al.*,²³ however, O_2^+ sputtering does not result in better resolved profiles than does Ar^+ sputtering, for Ni/Cr sandwiches. This fact may be explicable in terms of the growth of oxide crystallites on the O_2^+ -bombarded area. (The oxides of Ni and Cr are typical refractory ceramics.)

The fact that the nitrated zones on N_2^+ -sputtered Al and Mo were undetectable by TEM implies that the growth of AlN and Mo_2N layers was well balanced with the sputter removal of nitride molecules. At the present time, it is not possible to discuss why the growth of such a thin nitride layer led to a less-enhanced surface texturing. To answer this question, the underlying physical and chemical process in reactive N_2^+ sputtering must be elucidated.

Metal nitrides are typical interstitial compounds. In this kind of material, light atoms which diffuse into the mother lattice occupy interstitial positions. Since the atomic diffusion is a thermal process, an external heating is generally necessary to grow metal nitrides. The growth of nitride crystallites on N_2^+ -sputtered Ti and Ta in the present study is thus convincing evidence that the temperature of the ion-impacted area was elevated to a degree where the implanted nitrogen atoms were mobile. The ion-current density employed was as low as $100 \mu A/cm^2$, and the current consensus is that no thermal process should be involved in ion sputtering at such a low current density. In the light of our TEM data, this conventional view deserves careful reconsideration.

V. CONCLUDING REMARKS

The improvement in depth resolution associated with N_2^+ sputtering has been shown to be attainable, only when the nitride formation is confined to the surface or near-surface region. For materials which react with nitrogen so fast as to form bulk nitride, N_2^+ sputtering does not improve but compromises the resolution seriously. Furthermore, N_2^+ sputtering requires a long sputtering time for

one run of depth profiling, which is clearly undesirable from the practical point of view. Our conclusion is that N_2^+ sputtering is not a beneficial means to improve the practicality of Auger in-depth analysis.

Finally, it is emphasized once again that the heating up of the ion-impacted surface¹⁸ must be postulated to interpret the bulk-nitride formation on N_2^+ -sputtered Ti and Ta. To confirm this hypothesis, systematic experiments are now being undertaken, using the N_2^+/Ti system. The results will be dealt with in a forthcoming paper.

ACKNOWLEDGMENTS

Sincere thanks are expressed to Dr. Y. Taga for providing the samples. The competent assistance of Y. Fujimoto and K. Domaie is also gratefully acknowledged.

- ¹H. J. Mathieu, D. E. McClure, and D. Landolt, *Thin Solid Films* **38**, 281 (1976).
- ²M. P. Seah and C. P. Hunt, *Surf. Interface Anal.* **5**, 33 (1983).
- ³M. P. Seah and M. E. Jones, *Thin Solid Films* **115**, 203 (1984).
- ⁴D. F. Mitchell and G. I. Sproule, *Surf. Sci.* **117**, 238 (1986).
- ⁵M. Tanemura and F. Okuyama, *J. Vac. Sci. Technol. A* **4**, 2369 (1986).
- ⁶M. Tanemura, S. Fujimoto, and F. Okuyama, *Surf. Sci.* **230**, 283 (1990).
- ⁷M. Tanemura and F. Okuyama, *Thin Solid Films* **165**, 193 (1988).
- ⁸W. O. Hofer and H. Liebl, *Appl. Phys.* **8**, 359 (1975).
- ⁹H. M. Windawl, J. R. Katzer, and C. B. Cooper, *Phys. Lett.* **59A**, 62 (1976).
- ¹⁰R. J. Blattner, S. Nadel, C. A. Evans, Jr., A. J. Braundmeier, Jr., and C. W. Magee, *Surf. Interface Anal.* **1**, 32 (1979).
- ¹¹S. Hofmann and A. Zalar, *Thin Solid Films* **60**, 201 (1979).
- ¹²P. C. Zalm and L. J. Beckers, *J. Appl. Phys.* **56**, 220 (1984).
- ¹³*CRC Handbook of Chemistry and Physics*, edited by R. C. Weast and M. J. Astle (CRC Press, Boca Raton, 1980-1981), p. D-67.
- ¹⁴M. P. Seah and W. A. Dench, *Surf. Interface Anal.* **1**, 2 (1984).
- ¹⁵T. Sekine, Y. Nagasawa, M. Kudoh, Y. Sakai, A. S. Parkes, J. D. Geller, A. Mogami, and K. Hirata, in *Handbook of Auger Electron Spectroscopy* (JOEL Ltd., Tokyo, 1982).
- ¹⁶S. Hofmann, in *Practical Surface Analysis by Auger and X-ray Photoelectron Spectroscopy* (Wiley, Chichester, 1984), Chap. 4.
- ¹⁷K. Fujinaga and I. Kawashima, *J. Vac. Sci. Technol. A* **6**, 213 (1988).
- ¹⁸M. Tanemura and F. Okuyama, *Nucl. Instrum. Methods B* **47**, 126 (1990).
- ¹⁹C. D. Wagner, W. M. Riggs, L. E. Davis, J. F. Moulder, and G. E. Muilenberg, in *Handbook of X-Ray Photoelectron Spectroscopy* (Perkin-Elmer, Minnesota, 1979).
- ²⁰J. A. Taylor and J. W. Rabalais, *J. Chem. Phys.* **75**, 1735 (1981).
- ²¹P. Sigmund, in *Sputtering by Particle Bombardment*, edited by R. Behrisch (Springer, Berlin, 1981), Vol. 1, Chap. 2.
- ²²J. Lindhard, M. Scharff, and H. E. Schiøtt, *Mat-Fys-Medd. Dan. Vid. Selsk.* **33**, 14 (1963).
- ²³M. Moens, F. C. Adams, and D. S. Simons, *Anal. Chem.* **59**, 1518 (1987).